



Dalton
Transactions

Reactivity of molybdenum-nitride complex bearing pyridine-based PNP-type pincer ligand toward carbon-centred electrophiles

Journal:	<i>Dalton Transactions</i>
Manuscript ID	DT-ART-11-2021-003952.R1
Article Type:	Paper
Date Submitted by the Author:	20-Dec-2021
Complete List of Authors:	Itabashi, Takayuki; The University of Tokyo, School of Engineering, Arashiba, Kazuya; The University of Tokyo, School of Engineering, Kuriyama, Shogo; The University of Tokyo, School of Engineering, Nishibayashi, Yoshiaki; The University of Tokyo, School of Engineering,

SCHOLARONE™
Manuscripts

ARTICLE

Reactivity of molybdenum-nitride complex bearing pyridine-based PNP-type pincer ligand toward carbon-centered electrophiles

Received 00th January 20xx,
Accepted 00th January 20xx

DOI: 10.1039/x0xx00000x

Takayuki Itabashi, Kazuya Arashiba, Shogo Kuriyama, and Yoshiaki Nishibayashi*

A molybdenum-nitride complex bearing a pyridine-based PNP-type pincer ligand derived from dinitrogen is reacted with various kinds of carbon-centered electrophiles to functionalize the nitride ligand in the molybdenum complex. Methylation with MeOTf and acylation with diphenylacetyl chloride to the nitride complex afford the corresponding imide complexes via a carbon-nitrogen bond formation. In the case of reactions with phenylisocyanate and diphenylketene, the PNP ligand works as a non-innocent ligand to form the corresponding ureate and acylimide complexes, respectively. These newly synthesized complexes are characterized by X-ray analysis. As further transformation of the prepared imide complexes, hydrolysis of the molybdenum-acylimide complex proceeds to give the corresponding amide as an organonitrogen compound together with the corresponding molybdenum-oxo complex. This result indicates that nitrogen molecule is converted into organic amide mediated by the molybdenum-nitride complex.

Introduction

Organonitrogen chemicals such as nitrile rubbers, polyimide plastics, and pharmaceuticals are important materials that support our current life. Generally, the nitrogen source of these organonitrogen chemicals is supplied by ammonia produced from the Haber-Bosch process, where dinitrogen reacts with dihydrogen under harsh reaction conditions (high temperatures and high pressures).^{1–3} These harsh reaction conditions are necessary to overcome a high energy barrier of the dissociation of the nitrogen-nitrogen triple bond in dinitrogen molecule on catalyst surfaces. Besides, the production of dihydrogen by steam reforming of fossil fuels exhausts a large amount of carbon dioxide (about 0.8–1.5% of world total carbon dioxide emissions).^{4,5} As a result, the development of novel heterogeneous catalysts to reduce reaction temperatures and pressures and novel reaction systems to use green dihydrogen has been investigated for the last decade.^{6–8} On the other hand, the development of convenience synthesis of organonitrogen chemicals directly from dinitrogen also has a potential to avoid the consumption of fossil fuel.^{9–11}

In addition to the use of heterogeneous reaction systems, the development of homogeneous reaction systems using transition metal complexes as catalysts to produce ammonia under mild reaction conditions has been well investigated for the last two decades.^{12,13} In fact, several transition metal–dinitrogen complexes have been found to work as effective

catalysts toward the formation of ammonia and/or hydrazine under mild reaction conditions.^{14–23} Recently, we have achieved effective ammonia formation from dinitrogen catalysed by molybdenum complexes bearing a pyridine-based PNP-type pincer ligand under ambient reaction conditions (Scheme 1a).^{24,25} In this reaction system, molybdenum–nitride complex [Mo(N)I(PNP)] (PNP = 2,6-bis(di-*tert*-butylphosphinomethyl)pyridine) (**1**) generated by direct cleavage of the bridging dinitrogen on the dinitrogen-bridged dimolybdenum complex plays a key reactive intermediate to form ammonia followed by sequential protonation and reduction of the nitride complex. As an extensive work, more recently we have found more effective ammonia formation from the reaction of dinitrogen with samarium diiodide and water under ambient reaction conditions to afford over 4000 equiv of ammonia based on the molybdenum atom of the catalyst with the rate of 120 equiv of ammonia produced per minute based on the molybdenum atom of the catalyst.²⁶

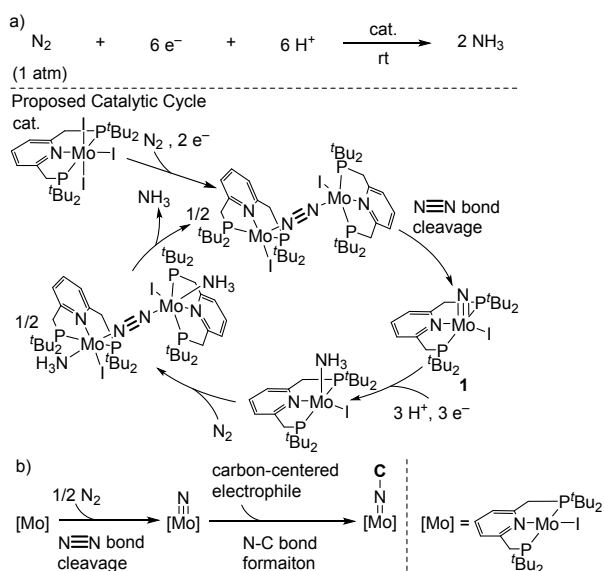
In 1995, Laplaza and Cummins reported the first successful example of direct cleavage of the bridging dinitrogen on dinitrogen-bridged dimolybdenum complex bearing triamide ligands [Mo(N^tBuAr)₃]₂(μ-N₂) (Ar = 3,5-dimethylphenyl) under mild reaction conditions to afford the corresponding molybdenum–nitride complex [Mo(N)(N^tBuAr)₃] in a high yield.^{27,28} After this milestone work, other research groups reported the formation of similar nitride complexes via direct cleavage of the bridging dinitrogen on dinitrogen-bridged dimetal complexes.^{29–42} Interestingly, Cummins and co-workers found the formation of nitriles from reactions of nitride complexes with acid chlorides.^{43–45} This research group successfully achieved a pseudo catalytic cycle to convert dinitrogen into nitriles with a stoichiometric amount of

Department of Applied Chemistry, School of Engineering, The University of Tokyo, Hongo, Bunkyo-ku, Tokyo 113-8656, Japan

* Electronic Supplementary Information (ESI) available: [details of any supplementary information available should be included here]. See DOI: 10.1039/x0xx00000x

transition metal complex.^{44,45} Based on this methodology, stepwise transformations of metal-nitride complexes into nitriles have been reported in a similar way by other research groups.^{37,46–48} These results open a new approach to prepare organonitrogen compounds directly from dinitrogen under mild reaction conditions although a stoichiometric amount of transition metal complexes is necessary to promote the corresponding pseudo catalytic cycles in all cases.

Based on these research backgrounds, we have envisaged that detailed investigations on the reactivity of the molybdenum–nitride complex [Mo(N)I(PNP)] **1** toward organic compounds may lead to the development of a new synthetic method for the preparation of organonitrogen compounds directly from dinitrogen under ambient reaction conditions. To achieve this goal, we have investigated reactions of **1** with various carbon-centred electrophiles under ambient reaction conditions to afford the corresponding molybdenum–imide complexes in good to high yields together with their structural analysis by X-ray analysis (Scheme 1b). Herein, we report typical results of stoichiometric reactions in details.



Scheme 1 (a) Catalytic ammonia formation via cleavage of dinitrogen. (b) Stoichiometric reactions of nitride complex with carbon-centered nucleophiles to afford the corresponding imide complexes.

Results and discussions

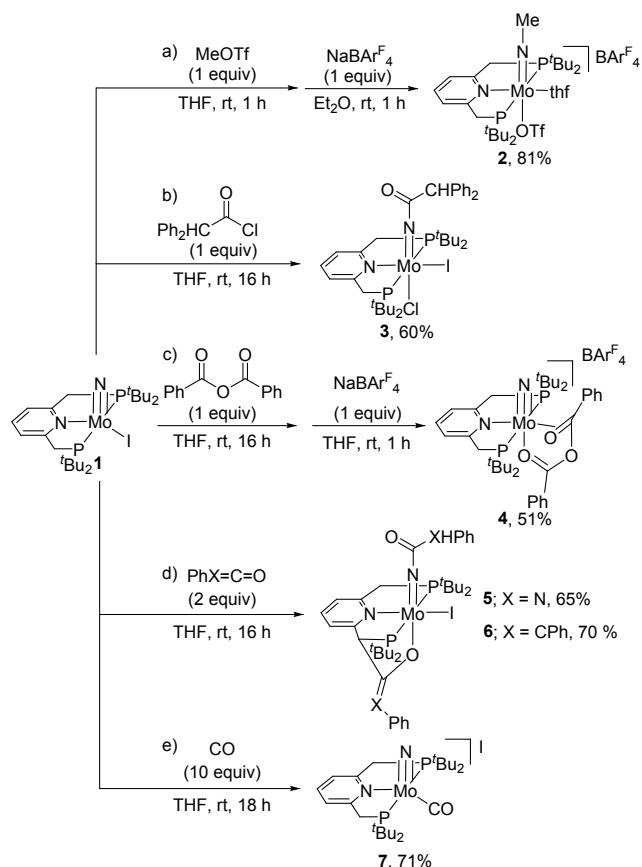
First, we carried out alkylation of the molybdenum–nitride complex **1** with a methylation reagent. Treatment of **1** with 2.0 equiv of MeOTf (OTf = trifluoromethylsulfonate) in THF at room temperature for 1 h under 1 atm of Ar afforded the corresponding methylimide complex [Mo(NMe)(THF)(OTf)(PNP)][BAR^F₄] (**2**) (Ar^F = 3,5-bis(trifluoromethyl)phenyl) in 81% yield after the addition of NaBAR^F₄ in Et₂O at room temperature for 1 h (Scheme 2a). The addition of NaBAR^F₄ to the reaction mixture is necessary to isolate the methylimide complex as a pure form. This methylimide complex was characterized by ¹H and ³¹P NMR. The presence of a methylimide ligand was supported by a

resonance for a methyl group at 3.65 ppm (t, $J_{H-P} = 2.1$ Hz). No further methylated complexes were observed by NMR in the crude reaction mixture.

A detailed molecular structure of this imide complex **2** was confirmed by X-ray analysis. An ORTEP drawing of **2** is shown in Fig. 1. Complex **2** has a distorted octahedral geometry around the molybdenum atom, where a methylimide ligand is coordinated to the molybdenum center with a Mo1-N2-C24 angle of 179.2(7)° in the apical position to the nitrogen atom of the pyridine ring. The bond distances between Mo1-N2 and N2-C24 are 1.721(6) Å and 1.445(11) Å, respectively, which are in typical bond ranges of molybdenum–alkylimide complexes.^{49,50} An OTf ligand and a THF molecule are located to the *trans*- and *cis*-positions to the methylimide ligand, respectively.

Next, we carried out acylation of **1** with carboxylic acid derivatives. The reaction of **1** with 1.1 equiv of 2,2-diphenylacetyl chloride in THF at room temperature for 16 h under 1 atm of Ar afforded the corresponding acylimide complex [Mo(NCOCHPh₂)Cl(PNP)] (**3**) in 60% yield (Scheme 2b). This acylimide complex was characterized by ¹H and ³¹P NMR. The IR absorption at 1628 cm⁻¹ derived from a C=O stretching vibration indicated the formation of an acylimide ligand.

A detailed molecular structure of this acylimide complex **3** was confirmed by X-ray analysis. An ORTEP drawing of **3** is shown in Fig. 2. Complex **3** has a distorted octahedral geometry around the molybdenum atom, where an acylimide ligand is coordinated to the molybdenum center with a Mo1-N2-C24 angle of 172.7(3)° in the apical position to the nitrogen atom of the pyridine ring. The bond distances between Mo1-N2 (1.768(3) Å) and N2-C24 (1.381(5) Å) in **3** are longer and shorter than those in **2**, respectively. This phenomenon is a typical feature of acylimide ligands.^{49,50} An iodo and a chloro ligands are presented in the *cis* and *trans* positions to the acylimide ligand, respectively.



Scheme 2 Reactions of **1** with carbon-centered electrophiles. (a) Reaction with MeOTf. (b) Reaction with Ph_2CHCOCl . (c) Reaction with Bz_2O . (d) Reactions with $\text{PhN}=\text{C}=\text{O}$ and $\text{Ph}_2\text{C}=\text{C}=\text{O}$. (e) Reaction with CO.

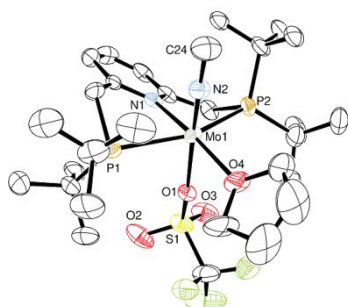


Fig. 1 An ORTEP drawing of **2**. Thermal ellipsoids are shown at the 50% probability level. All hydrogen atoms as well as BARF_4 anion are omitted for clarity.

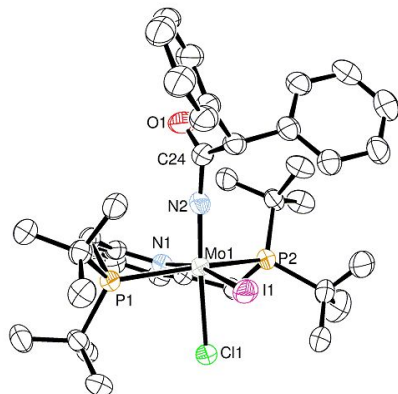


Fig. 2 An ORTEP drawing of **3**. Thermal ellipsoids are shown at the 50% probability level. All hydrogen atoms are omitted for clarity.

The reaction of **1** with 1 equiv of benzoic anhydride (Bz_2O) in THF at room temperature for 16 h under 1 atm of Ar afforded the corresponding nitride complex $[\text{Mo}(\text{N})(\eta^3\text{-Bz}_2\text{O})(\text{PNP})][\text{BARF}_4]$ (**4**) in 51% yield after the addition of NaBARF_4 in THF at room temperature for 1 h (Scheme 2c). The asymmetrical coordination of one Bz_2O molecule to the molybdenum center was confirmed by ^1H and ^{31}P NMR.

A detailed molecular structure of this imide complex **4** was confirmed by X-ray analysis. An ORTEP drawing of **4** is shown in Fig. 3. Complex **4** has a distorted octahedral geometry around the molybdenum atom, where one Bz_2O molecule is coordinated to the molybdenum atom with two carbonyl groups, one carbonyl group is bounded with an oxygen atom and the other carbonyl group is bounded with a $\text{C}=\text{O}$ double bond. It is noteworthy that no acylation of the nitride complex **1** occurred at all under the present reaction conditions. The bond length of the nitride ligand in **4** (1.654(5) Å) is almost the same with that in **1** (1.685(3) Å).

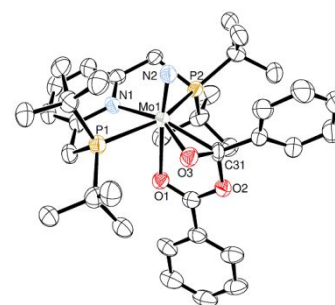


Fig. 3 An ORTEP drawing of **4**. Thermal ellipsoids are shown at the 50% probability level. All hydrogen atoms as well as BARF_4 anion are omitted for clarity.

The reaction of **1** with 2 equiv of phenylisocyanate ($\text{PhN}=\text{C}=\text{O}$) in THF at room temperature for 16 h under 1 atm of Ar gave the corresponding ureate complex (**5**) in 65% yield (Scheme 2d). ^1H and ^{31}P NMR spectra of the complex suggests an asymmetrical structure of the PNP-type pincer ligand. In the ^1H NMR spectrum, a resonance for N-H bond in the ureate ligand was observed at 8.96 ppm in $\text{THF-}d_8$.

A detailed molecular structure of this ureate complex **5** was confirmed by X-ray analysis. An ORTEP drawing of **5** is shown in Fig 4, left. Complex **5** has a distorted octahedral geometry around the molybdenum atom, where two PhNCO molecules are added to the molybdenum-nitride complex **1**. An ureate ligand is coordinated to the molybdenum center with a Mo1-N2-C24 angle of $164.9(2)^\circ$ in the apical position to the nitrogen atom of the pyridine ring, where the bond distances between Mo1-N2 and N2-C24 are 1.755(3) Å and 1.394(4) Å, respectively, which are in typical bond ranges of metal-ureate complexes.^{51,52} On the other hand, the bond lengths of C31-N4 (1.283(4) Å), C31-O2 (1.317(4) Å), and Mo1-O2 (2.115(2) Å) are indicating the coordination of an imidate ligand to the molybdenum atom. These results suggest that nucleophilic attack of nitride ligand of **1** to the first PhNCO molecule occurs together with the deprotonation of benzylic proton of the PNP-type pincer ligand with the formed ureate ligand, then the second PhNCO

molecule is coordinated to the molybdenum-ureate complex bearing a dearomatized PNP-type pincer ligand to form a carbon-carbon single bond C1-C31 (1.532(4) Å) and a molybdenum-oxygen single bond Mo1-O2 (2.115(2) Å) as an imidate ligand (Fig 4, left). An iodo ligand is presented in the *trans* position to the nitrogen atom of the PNP-type pincer ligand.

When the reaction of **1** with 2 equiv of diphenylketene (Ph₂C=C=O), in place of PhN=C=O, was carried out under the same reaction conditions, a similar acylimide complex **6** bearing an enolate ligand was obtained in 70% yield (Scheme 2d). A detailed molecular structure of this imide complex **6** was confirmed by X-ray analysis. An ORTEP drawing of **6** is shown in Fig. 4, right.

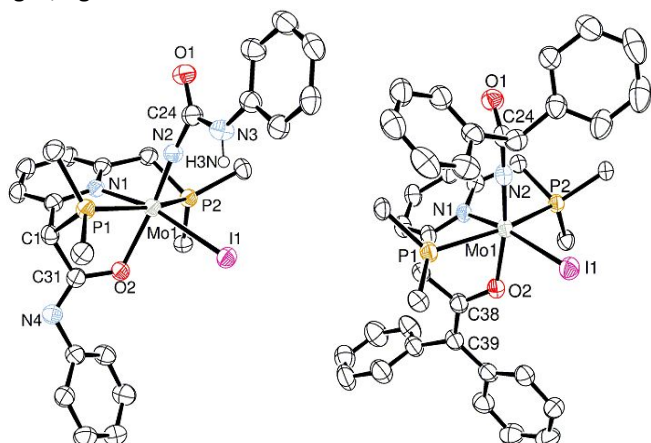


Fig. 4 ORTEP drawings of **5** (left) and **6** (right). Thermal ellipsoids are shown at the 50% probability level. All hydrogen atoms except for H3N, solvent molecules as well as methyl groups of ^tBu groups are omitted for clarity.

The reaction of **1** with an excess amount (10 equiv) of carbon monoxide (CO) in THF at room temperature for 16 h gave the corresponding cationic nitride carbonyl complex [Mo(N)(CO)(PNP)]⁺[I]⁻ (**7**) in 76% yield (Scheme 2e). This cationic complex was characterized by ¹H and ³¹P NMR and IR spectroscopies. ¹H and ³¹P{¹H} NMR spectra of **7** suggest a C_s symmetric structure in solution. IR spectrum shows a strong absorption at 1954 cm⁻¹, indicating the presence of CO ligand.

A detailed molecular structure of the cationic nitride carbonyl complex **7** was confirmed by X-ray analysis. An ORTEP drawing of **7** is shown in Fig. 5. Complex **7** has a distorted square-pyramidal geometry around the molybdenum atom with the PNP and CO ligands in the basal plane and the nitride ligand in the apical position ($\tau = 0.254$).⁵³ The bond distances and angles of **7** are almost the same with that of the starting nitride complex **1**, where the iodide ligand is replaced with CO ligand and the iodide moiety is presented as a counter anion.

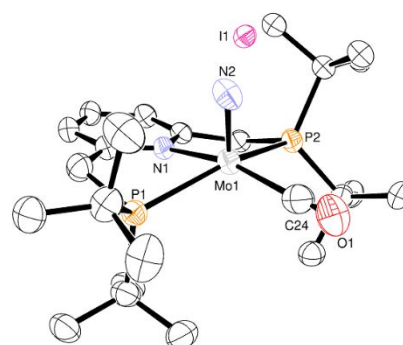
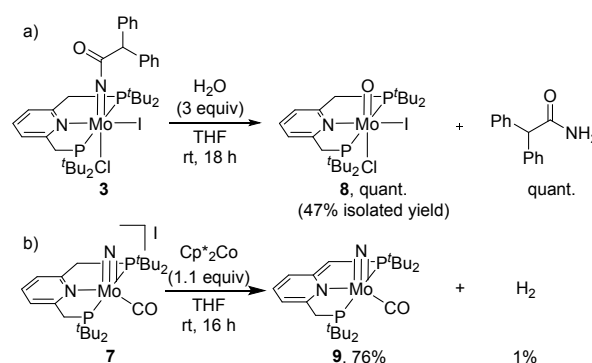


Fig. 5 An ORTEP drawings of **7**. Thermal ellipsoids are shown at the 50% probability level. All hydrogen atoms as well as solvent molecules are omitted for clarity.

Finally, we investigated the reactivity of the identified complexes produced from reactions of **1** with various carbon-centered electrophiles. The reaction of the acylimide complex **3** with 3 equiv of water (H₂O) in THF at room temperature for 18 h under 1 atm of Ar afforded the corresponding oxo complex [Mo(O)Cl(PNP)] (**8**) and 2,2-diphenylacetoamide quantitatively (Scheme 3a). The NMR yields of **8** and amide were determined by ¹H NMR from the reaction mixture. After recrystallization of the crude reaction mixture, the oxo complex **8** was isolated in 47% yield.

A detailed molecular structure of the oxo complex **8** was confirmed by X-ray analysis. An ORTEP drawing of **8** is shown in Fig. 6. Complex **8** has a distorted octahedral geometry around the molybdenum atom, where an oxo ligand is coordinated to the molybdenum center in the apical position to the nitrogen atom of the pyridine ring. The bond distance between Mo1-O1 is 1.870(5) Å is slightly longer than a typical bond range of molybdenum–oxo complexes.^{26,54} A chloride ligand and an iodide molecular are located to the *trans*- and *cis*-positions to the oxo ligand, respectively.

The acylimide moiety of **3** was successfully converted into amide in a quantitative yield. This experimental result indicates that nitrogen molecule is converted into a typical organonitrogen compound such as an organic amide via the molybdenum–nitride complex which can be prepared from direct cleavage of the dinitrogen-bridging ligand of the dinitrogen-bridged dimolybdenum complex.



Scheme 3 (a) Hydrolysis of **3**. (b) Reduction of **7**.

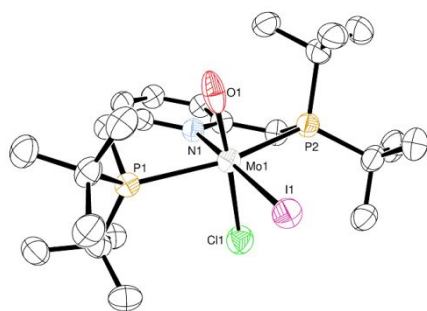


Fig. 6 An ORTEP drawings of **8**. Thermal ellipsoids are shown at the 50% probability level. All hydrogen atoms are omitted for clarity.

The reaction of the nitride carbonyl complex $[\text{Mo}(\text{N})(\text{CO})(\text{PNP})][\text{I}]$ **7** with 1.1 equiv of decamethylcobaltocene (CoCp^*_2 ; $\text{Cp}^* = \eta^5\text{-C}_5\text{Me}_5$) as a reductant in THF at room temperature for 16 h under 1 atm of Ar afforded the corresponding neutral nitride carbonyl complex bearing a dearomatized PNP-type pincer ligand $[\text{Mo}(\text{N})(\text{CO})(\text{PNP}')] (\mathbf{9})$ ($\text{PNP}' =$ dearomatized PNP-type pincer ligand) in 76% yield (Scheme 3b). In this reaction, only a small amount of dihydrogen (0.01 equiv/Mo) was detected after the reaction. An asymmetrical structure of the PNP-type pincer ligand was confirmed by ^{31}P NMR spectroscopy. ^1H NMR spectra indicates that deprotonation at the benzylic position of the PNP ligand promoted dearomatization of the pyridine ring. A red-shifted absorbance was observed when we compared a CO stretching vibration of **9** (1930 cm^{-1}) with that of **7** (1954 cm^{-1}). We consider that this red-shift is due to the strong electron donating ability derived from the dearomatized PNP ligand. Although detailed reaction mechanism of this reaction is unclear, we consider one possibility of deprotonation at the benzylic proton in the PNP ligand with one-electron reduced nitride carbonyl complex to afford **9** after dehydrogenation.

A detailed molecular structure of the neutral nitride carbonyl complex **9** was confirmed by X-ray analysis. An ORTEP drawing of **9** is shown in Fig. 7. Complex **9** has a distorted square-pyramidal geometry around the molybdenum atom with the dearomatized PNP and CO ligands in the basal plane and the nitride ligand in the apical position ($\tau = 0.072$).⁵³ The bond length of the nitride ligand in **9** ($1.660(4)\text{ \AA}$) is almost the same with that in **7** ($1.634(4)\text{ \AA}$). The deprotonation of benzylic proton of the PNP-type pincer ligand is supported by a carbon-carbon double bond between C6 and C7 ($1.386(7)\text{ \AA}$).

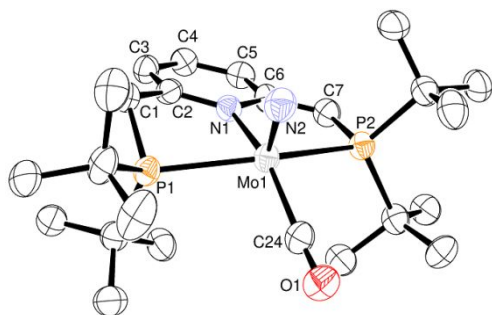
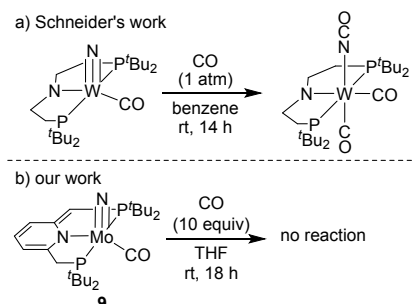


Fig. 7 An ORTEP drawings of **9**. Thermal ellipsoids are shown at the 50% probability level. All hydrogen atoms are omitted for clarity.

Schneider and co-workers reported that the reaction of a tungsten nitride carbonyl complex bearing an amide-type $\text{PN}^{\text{amide}}\text{P}$ pincer ligand $[\text{W}(\text{N})(\text{CO})\text{PN}^{\text{amide}}\text{P}]$ ($\text{PN}^{\text{amide}}\text{P} =$ bis(di-*tert*-butylphosphinoethyl)amide) with CO to give the corresponding tungsten isocyanate dicarbonyl complex $[\text{W}(\text{NCO})(\text{CO})_2\text{PN}^{\text{amide}}\text{P}]$ (Scheme 4a).⁴² On the other hand, no reaction of **9** with CO was observed although the reaction conditions are quite different from those of the reaction with tungsten nitride carbonyl complex (Scheme 4b).



Scheme 4 (a) Carbonylation of tungsten nitride carbonyl complex.⁴² (b) Trial of carbonylation of **9**.

Conclusions

We have investigated the reactivity of molybdenum-nitride complex, which can be prepared directly from dinitrogen under ambient reaction conditions, with various carbon-centered electrophiles. Methylation with MeOTf and acylation with diphenylacetyl chloride to the nitride complex afforded the corresponding imide complexes. In reactions with phenylisocyanate and diphenylketene, the PNP ligand worked as a non-innocent ligand to form the corresponding ureate and acylimide complexes, respectively. On the other hand, in reactions with benzoic anhydride and carbon monoxide, these molecules were coordinated to the molybdenum center rather than reacted with the nitride ligand. As further transformation of the prepared imide complexes, hydrolysis of the molybdenum-acylimide complex gave an organic amide together with the corresponding molybdenum-oxo complex. This result indicates that the nitrogen molecule is converted into organic amide mediated by the molybdenum-nitride complex. We believe that these experimental results shown in this manuscript provide useful information to develop catalytic synthesis of organonitrogen compounds directly from dinitrogen under mild reaction conditions. Quite recently, Mézailles and co-workers reported the reaction of anionic molybdenum-nitride complex bearing a POCOP-type pincer ligand $[\text{Na}][\text{Mo}(\text{N})\text{I}(\text{POCOP})]$ (POCOP = 2,6-bis(di-*tert*-butylphosphinoxy)phenyl) toward alkyne to give the corresponding nitriles via cross-metathesis between the nitride ligand and alkynes.⁵⁵ Further study on transformation of nitride complexes with carbon sources such as alkynes and alkenes is currently underway.

Experimental section

General Methods. ^1H NMR (400 MHz), ^{19}F NMR (376 MHz), and $^{31}\text{P}\{^1\text{H}\}$ NMR (162 MHz) spectra were recorded on a JEOL ECS-400 spectrometer in suitable solvent, and spectra were referenced to residual solvent (^1H) or external standard (^{19}F : $\text{BF}_3 \cdot \text{Et}_2\text{O}$, $^{31}\text{P}\{^1\text{H}\}$: H_3PO_4). Evolved dihydrogen was quantified by a gas chromatography using a Shimadzu GC-8A with a TCD detector and a SHINCARBON ST (6 m \times 3 mm). IR spectra were recorded on a JASCO FT/IR 4100 Fourier Transform infrared spectrometer. Elemental analyses were performed at Microanalytical Center of The University of Tokyo. All manipulations were carried out under an atmosphere of nitrogen by using standard Schlenk techniques or glovebox techniques unless otherwise stated. Solvents were dried by general methods and degassed before use. $[\text{Mo}(\text{N})(\text{PNP})]$ (**1**),²⁴ $\text{NaBAR}^{\text{F}_4}$,⁵⁶ and CoCp^*_{257} were prepared according to the literature methods. Other reagents were purchased commercially and used as received.

Synthesis of $[\text{Mo}(\text{NMe})(\text{THF})(\text{OTf})(\text{PNP})][\text{BAR}^{\text{F}_4}]$ (2**).** To a THF (3 mL) solution of **1** (19.1 mg, 0.0302 mmol) was added MeOTf (10.2 μL , 0.0622 mmol) under Ar (1 atm). After stirring at rt for 1 h, volatiles were removed *in vacuo*. To the residue were added $\text{NaBAR}^{\text{F}_4}$ (25.2 mg, 0.0284 mmol) and Et_2O (2 mL), and then the mixture was stirred at rt for 1 h. The resultant green solution was filtered through Celite, and the filter cake was washed with ether (1 mL \times 2). After the combined filtrate was concentrated, slow addition of hexane (10 mL) afforded **2** as green crystals, which were collected by filtration, washed with hexane (1 mL \times 3), and dried *in vacuo* (37.1 mg, 0.0231 mmol, 81% yield). In the ^1H NMR measurement in CD_3CN , ligand exchange between THF and CD_3CN was observed. ^1H NMR (CD_3CN): δ 7.92 (t, $J = 7.8$ Hz, ArH, 1H), 7.68 (s, Ar^{F_4} , 8H), 7.66 (s, Ar^{F_4} , 4H), 7.52 (d, $J = 7.8$ Hz, ArH, 2H), 3.79 (pseudo t, $J = 3.2$ Hz, CH_2P , 4H), 3.65 (t, $J = 2.1$ Hz, NMe, 3H), 1.33 (pseudo t, $J = 6.9$ Hz, P^{tBu_2} , 36H). $^{31}\text{P}\{^1\text{H}\}$ NMR (CD_3CN): δ 81.3 (s). ^{19}F NMR (CD_3CN): δ -63.2 (s, Ar^{F_4}), -79.2 (s, OTf). Anal. Calcd. for $\text{C}_{61}\text{H}_{66}\text{BF}_{27}\text{MoN}_2\text{O}_4\text{P}_2\text{S}$: C, 45.65; H, 4.15; N, 1.75. Found: C, 45.37; H, 4.14; N, 1.89.

Synthesis of complex $[\text{Mo}(\text{NCOCHPh}_2)\text{ICl}(\text{PNP})]$ (3**).** A mixture of **1** (50.1 mg, 0.0792 mmol) and diphenylacetylchloride (19.5 mg, 0.0845 mmol) in THF (10 mL) was stirred at rt for 16 h. After the reaction, the solution was filtered through Celite, and the filter cake was washed with THF (1 mL). After the combined filtrate was concentrated, slow addition of hexane (20 mL) afforded **3** \cdot 0.5THF as orange crystals, which were collected by filtration, washed with Et_2O (3 mL \times 3), and dried *in vacuo* (43.0 mg, 0.0478 mmol, 60% yield). ^1H NMR (THF- d_6): 7.70-7.66 (m, ArH, 3H), 7.59 (d, $J = 7.3$ Hz, ArH, 4H), 7.14 (t, $J = 7.6$ Hz, ArH, 4H), 7.06 (t, $J = 7.3$ Hz, ArH, 2H), 6.08 (s, NCHPh₂, 1H), 4.28 (d, $J = 15.1$ Hz, CH_2P , 2H), 3.90 (d, $J = 16.0$ Hz, CH_2P , 2H), 1.46 (br s, P^{tBu_2} , 18H), 0.93 (br s, P^{tBu_2} , 18H). $^{31}\text{P}\{^1\text{H}\}$ NMR (THF- d_6): δ 64.9 (s). IR (KBr): 1628 cm^{-1} (ν_{CO}). Anal. Calcd. for $\text{C}_{37}\text{H}_{54}\text{ClImoN}_2\text{OP}_2 \cdot 0.5\text{THF}$: C, 52.10; H, 6.50; N, 3.12. Found: C, 52.01; H, 6.65; N, 2.93.

Synthesis of complex $[\text{PNPMo}(\text{N})(\eta^3\text{-Bz}_2\text{O})][\text{BAR}^{\text{F}_4}]$ (4**).** A mixture of **1** (32.0 mg, 0.0506 mmol) and Bz_2O (12.0 mg, 0.0530 mmol) in THF (5 mL) was stirred at rt for 16h. To the resultant solution was added $\text{NaBAR}^{\text{F}_4}$ (43.8 mg, 0.0494 mmol), and then the mixture was stirred at

rt for 1 h. Volatiles were removed *in vacuo*, and Et_2O (3 mL) was added to the residue. The ether solution was filtered through Celite, and the filter cake was washed with ether (1 mL \times 2). After the combined filtrate was concentrated, slow addition of hexane (15 mL) afforded **4** as brown crystals, which were collected by filtration, washed with pentane (1 mL \times 3), and dried *in vacuo* (39.8 mg, 0.0250 mmol, 51% yield). ^1H NMR (THF- d_6): δ 8.16 (t, $J = 8.0$ Hz, 1H, ArH), 7.94 (d, $J = 7.3$ Hz, 2H, ArH), 7.88-7.81 (m, 4H, ArH), 7.79 (s, 8H, Ar^{F_4}), 7.68 (t, $J = 8.0$ Hz, 1H, ArH), 7.57 (s, 4H, Ar^{F_4}), 7.50-7.43 (m, 4H, ArH), 7.32 (t, $J = 7.3$ Hz, 1H, ArH), 4.27-4.03 (m, 4H, CH_2P), 1.51 (d, $J = 13.7$ Hz, 18H, P^{tBu_2}), 1.16 (d, $J = 14.2$ Hz, 9H, P^{tBu_2}), 0.96 (d, $J = 12.3$ Hz, 9H, P^{tBu_2}). $^{31}\text{P}\{^1\text{H}\}$ NMR (THF- d_6): δ 77.1 (d, $J = 69.5$ Hz), 67.8 (d, $J = 69.5$ Hz). IR (KBr): 1638 (ν_{CO}) cm^{-1} . Anal. Calcd. for $\text{C}_{69}\text{H}_{65}\text{BF}_{24}\text{MoN}_2\text{O}_3\text{P}_2$: C, 51.96; H, 4.11; N, 1.76. Found: C, 51.84; H, 4.03; N, 1.67.

Synthesis of complex **5.** A mixture of **1** (31.7 mg, 0.0501 mmol) and PhNCO (12.2 mg, 0.102 mmol) in THF (5 mL) was stirred at rt for 16 h. After volatiles were removed *in vacuo*, THF (2 mL) was added to the residue. The THF solution was filtered through Celite, and the filter cake was washed with THF (1 mL). After the combined filtrate was concentrated, slow addition of hexane (9 mL) afforded **5** \cdot THF as green crystals, which were collected by filtration, washed with pentane (1 mL \times 3), and dried *in vacuo* (30.7 mg, 0.0326 mmol, 65% yield). ^1H NMR (THF- d_6): δ 8.96 (s, 1H, CONHPh), 7.90-7.83 (m, 2H, ArH), 7.75 (d, $J = 7.3$ Hz, 1H, ArH), 7.47 (d, $J = 8.7$ Hz, 2H, ArH), 7.21 (t, $J = 7.8$ Hz, 2H, ArH), 6.99-6.91 (m, 5H, ArH), 6.70 (t, $J = 6.9$ Hz, 1H, ArH), 5.17 (d, $J = 6.4$ Hz, 1H, CHP), 4.28 (dd, $J = 16.0, 10.5$ Hz, 1H, CH_2P), 3.81 (dd, $J = 16.0, 5.0$ Hz, 1H, CH_2P), 1.80 (d, $J = 12.8$ Hz, 9H, P^{tBu_2}), 1.52 (d, $J = 13.3$ Hz, 9H, P^{tBu_2}), 1.06 (d, $J = 11.4$ Hz, 9H, P^{tBu_2}), 0.77 (d, $J = 12.8$ Hz, 9H, P^{tBu_2}). $^{31}\text{P}\{^1\text{H}\}$ NMR (THF- d_6): δ 104.7 (d, $J = 195.2$ Hz), 93.5 (d, $J = 195.2$ Hz). IR (KBr): 3244 cm^{-1} (ν_{NH}), 1671 cm^{-1} (ν_{CO}). Anal. Calcd. for $\text{C}_{37}\text{H}_{53}\text{ImoN}_4\text{O}_2\text{P}_2 \cdot \text{THF}$: C, 52.23; H, 6.52; N, 5.94. Found: C, 52.35; H, 6.20; N, 5.85.

Synthesis of complex **6.** A mixture of **1** (31.5 mg, 0.0498 mmol) and $\text{Ph}_2\text{C}=\text{C}=\text{O}$ (20.8 mg, 0.107 mmol) in THF (2.5 mL) was stirred at rt for 16 h. The brown solution was filtered through Celite, and the filter cake was washed with THF (1 mL). After the combined filtrate was concentrated, slow addition of hexane (6 mL) afforded **6** as brown crystals, which were collected by filtration, washed with pentane (1 mL \times 3), and dried *in vacuo* (35.4 mg, 0.0347 mmol, 70% yield). ^1H NMR (THF- d_6): δ 7.76 (t, $J = 3.0$ Hz, 2H, ArH), 7.57 (t, $J = 7.8$ Hz, 4H, ArH), 7.36 (t, $J = 7.1$ Hz, 3H, ArH), 7.29 (t, $J = 7.5$ Hz, 2H, ArH), 7.18-7.13 (m, 6H, ArH), 7.08 (t, $J = 6.9$ Hz, 2H, ArH), 7.02 (d, $J = 6.9$ Hz, 2H, ArH), 6.89 (t, $J = 7.5$ Hz, 2H, ArH), 6.77 (t, $J = 7.3$ Hz, 1H, ArH), 5.79 (s, 1H, COCHPh₂), 4.69 (d, $J = 6.9$ Hz, 1H, CHP), 4.32 (dd, $J = 15.6, 10.1$ Hz, 1H, CH_2P), 3.88 (dd, $J = 15.6, 5.0$ Hz, 1H, CH_2P), 1.78 (d, $J = 12.3$ Hz, 9H, P^{tBu_2}), 1.29 (d, $J = 12.8$ Hz, 9H, P^{tBu_2}), 0.76 (d, $J = 12.3$ Hz, 9H, P^{tBu_2}), 0.45 (d, $J = 11.4$ Hz, 9H, P^{tBu_2}). $^{31}\text{P}\{^1\text{H}\}$ NMR (THF- d_6): δ 103.0 (d, $J = 212.5$ Hz), 94.0 (d, $J = 212.5$ Hz). IR (KBr): 1634 cm^{-1} (ν_{CO}). Anal. Calcd. for $\text{C}_{51}\text{H}_{63}\text{ImoN}_2\text{P}_2$: C, 60.00; H, 6.22; N, 2.74. Found: C, 59.61; H, 6.16; N, 2.58.

Synthesis of $[\text{Mo}(\text{N})(\text{CO})(\text{PNP})][\text{I}]$ (7**).** To one side of bifurcated schlenk was added **1** (61.0 mg, 0.096 mmol) and THF (10 mL). To the other side of bifurcated Schlenk was added 2,4,6-trichlorophenyl

formate (224 mg, 0.994 mmol), THF (5 mL), and pyridine (50 μ L) in that order. After addition of pyridine, the bifurcated Schlenk was sealed and stirred at rt for 16 h. The red solution was concentrated under reduced pressure. The residue was dissolved in THF (5 mL), slow addition of hexane (25 mL) afforded **7** as pink crystals, which were collected by filtration, washed with ether (2 mL x 3), and dried *in vacuo* (48.2 mg, 0.728 mmol, 76% yield). $^1\text{H NMR}$ (THF- d_8): δ 7.93 (t, J = 7.8 Hz, ArH, 1H), 7.82 (d, J = 7.8 Hz, ArH, 2H), 4.44 (dt, J = 16.5, 3.7 Hz, CH_2P , 2H), 4.08 (dt, J = 16.5, 3.2 Hz, CH_2P , 2H), 1.47 (pseudo t, J = 6.8 Hz, P^iBu_2 , 18H), 1.39 (pseudo t, J = 6.8 Hz, P^iBu_2 , 18H). $^{31}\text{P}\{^1\text{H}\}$ NMR (THF- d_8): δ 78.6 (s). IR (KBr): 1954 cm^{-1} (ν_{CO}). Anal. Calcd. for $\text{C}_{24}\text{H}_{43}\text{IMoN}_2\text{OP}_2$: C, 43.65; H, 6.56; N, 4.24. Found: C, 43.73; H, 6.28; N, 4.13.

Hydrolysis of complex 3. To a THF solution of **3** (27.8 mg, 0.0322 mmol) was added H_2O (1 M in THF, 100 μ L, 0.10 mmol), and the mixture was stirred at rt for 18 h. After the reaction, volatiles were removed *in vacuo*. Quantitative formation of $[\text{Mo}(\text{O})\text{Cl}(\text{PNP})]$ (**8**) and diphenylacetamide were confirmed by $^1\text{H NMR}$ in THF- d_8 with hexamethylbenzene as an internal standard. Then, THF (2 mL) was added to the residue. The solution was filtered through Celite, and the filter cake was washed with THF (1 mL). After the combined filtrate was concentrated, slow addition of hexane (6 mL) afforded **7** as green crystals, which were collected by filtration, washed with ether (1 mL x 3), and dried *in vacuo* (11.2 mg, 0.0151 mmol, 47% yield).

Data for **8**. $^1\text{H NMR}$ (THF- d_8): δ 7.83 (t, J = 7.8 Hz, 1H, ArH), 7.71 (d, J = 7.8 Hz, 2H, ArH), 4.18 (dt, J = 16.2, 4.3 Hz, 2H, CH_2P), 3.88 (dt, J = 16.2, 3.9 Hz, 2H, CH_2P), 1.47 (t, J = 6.4 Hz, 18H, P^iBu_2), 1.40 (t, J = 6.2 Hz, 18H, P^iBu_2). $^{31}\text{P}\{^1\text{H}\}$ NMR (THF- d_8): δ 64.3 (s). Anal. Calcd. for $\text{C}_{23}\text{H}_{43}\text{ClIMoNOP}_2$: C, 41.24; H, 6.47; N, 2.09. Found: C, 41.38; H, 6.38; N, 1.75.

Synthesis of $[\text{Mo}(\text{N})(\text{CO})(\text{PNP}')]$ (9**).** A mixture of **7** (29.1 mg, 0.044 mmol) and CoCp^*_2 (15.1 mg, 0.046 mmol) in THF solution was stirred at rt for 16 h. After volatiles were removed *in vacuo*, pentane (2 mL) was added to the residue. The pentane solution was filtered through Celite, and the filter cake was washed with pentane (1 mL x 2). After the filtrate was combined, slow evaporation of pentane at -30°C afforded **9** as red crystals, which were collected by filtration, washed with cold pentane (0.5 mL), and dried *in vacuo* (17.8 mg, 0.033 mmol, 76% yield). $^1\text{H NMR}$ (C_6D_6): δ 6.47 (d, J = 8.7 Hz, $\text{C}_5\text{H}_3\text{N}$, 1H), 6.42–6.38 (m, $\text{C}_5\text{H}_3\text{N}$, 1H), 5.49 (d, J = 6.4 Hz, $\text{C}_5\text{H}_3\text{N}$, 1H), 3.81 (s, CHP , 1H), 3.14 (dd, J = 15.6, 6.4 Hz, CH_2P , 1H), 2.69 (dd, J = 15.6, 11.0 Hz, CH_2P , 1H), 1.63 (d, J = 13.7 Hz, P^iBu_2 , 9H), 1.25 (d, J = 13.7 Hz, P^iBu_2 , 9H), 1.07 (d, J = 13.7 Hz, P^iBu_2 , 9H), 0.71 (d, J = 12.8 Hz, P^iBu_2 , 9H). $^{31}\text{P}\{^1\text{H}\}$ NMR (THF- d_8): δ 84.0 (d, J = 82.4 Hz), 75.2 (d, J = 78.1 Hz). IR (KBr): 1930 cm^{-1} (ν_{CO}). Anal. Calcd. for $\text{C}_{24}\text{H}_{42}\text{MoN}_2\text{OP}_2$: C, 54.13; H, 7.95; N, 5.26. Found: C, 54.43; H, 7.88; N, 4.98.

X-ray crystallography. Diffraction data for **2** (CCDC 2123058), **3** (CCDC 2123059), **4** (CCDC 2123060), **5**-THF (CCDC 2123061), **6** (CCDC 2123062), **7** (CCDC 2123063), **8** (CCDC 2123064), and **9** (CCDC 2123065) were collected for the 2θ range of 4° to 63° at -180°C on a Rigaku XtaLAB Synergy-S diffractometer equipped with a HyPix-6000HE Hybrid Photon Counting (HPC) detector and VariMax optics using multi-layer mirror monochromated Mo $K\alpha$ radiation ($\lambda =$

0.71073 Å). Intensity data were corrected for Lorenz-polarization effects and for empirical absorption (CrysAlisPro),⁵⁸ whereas structure solutions and refinements were carried out by using the *CrystalStructure* crystallographic software package.⁵⁹ Positions of non-hydrogen atoms were determined by direct methods (SHELXS Version 2013/1 for **2**, **3**, **4**, **5**-THF, **6**, **7**, and **8**; SHELXT Version 2014/5 for **9**)^{60,61} and subsequent Fourier syntheses (SHELXL Version 2016/6),⁶² and were refined on F_o^2 using all unique reflections by full-matrix least-squares with anisotropic thermal parameters. All the hydrogen atoms except for the H(H3N) atom in **5**-THF were placed at the calculated positions with fixed isotropic parameters. The position of the H(H3N) atom in **5**-THF was determined on the peak in the difference Fourier maps and further refined isotropically. Details of the crystallographic data are summarized in the Supplementary Information.

Conflicts of interest

There are no conflicts to declare.

Acknowledgements

The present project is supported by CREST, JST (JPMJCR1541). We thank Grants-in-Aids for Scientific Research (Nos. JP20H05671 and 20K21203) from JSPS. T.I. is a recipient of the JSPS Predoctoral Fellowships for Young Scientists.

References

- M. Appl, in *Ullmann's Encyclopedia of Industrial Chemistry*, ed. Wiley-VCH Verlag GmbH & Co. KGaA, Wiley-VCH Verlag GmbH & Co. KGaA, Weinheim, Germany, 2011, p. a02_143.pub3.
- M. Appl, in *Ullmann's Encyclopedia of Industrial Chemistry*, ed. Wiley-VCH Verlag GmbH & Co. KGaA, Wiley-VCH Verlag GmbH & Co. KGaA, Weinheim, Germany, 2011, p. o02_o11.
- M. Appl, in *Ullmann's Encyclopedia of Industrial Chemistry*, ed. Wiley-VCH Verlag GmbH & Co. KGaA, Wiley-VCH Verlag GmbH & Co. KGaA, Weinheim, Germany, 2011, p. o02_o12.
- P. G. Levi and J. M. Cullen, *Environ. Sci. Technol.*, 2018, **52**, 1725–1734.
- L. Boerner Krietsch, *Chem. Eng. News*, 2019, **97**, 18–23.
- H. Hosono and M. Kitano, *Chem. Rev.*, 2021, **121**, 3121–3185.
- R. Shi, X. Zhang, G. I. N. Waterhouse, Y. Zhao and T. Zhang, *Adv. Energy Mater.*, 2020, **10**, 2000659.
- M. Torimoto, K. Murakami and Y. Sekine, *Bull. Chem. Soc. Jpn.*, 2019, **92**, 1785–1792.
- C. Chen, X. Zhu, X. Wen, Y. Zhou, L. Zhou, H. Li, L. Tao, Q. Li, S. Du, T. Liu, D. Yan, C. Xie, Y. Zou, Y. Wang, R. Chen, J. Huo, Y. Li, J. Cheng, H. Su, X. Zhao, W. Cheng, Q. Liu, H. Lin, J. Luo, J. Chen, M. Dong, K. Cheng, C. Li and S. Wang, *Nat. Chem.*, 2020, **12**, 717–724.
- M. Yuan, J. Chen, Y. Bai, Z. Liu, J. Zhang, T. Zhao, Q. Wang, S. Li, H. He and G. Zhang, *Angew. Chem. Int. Ed.*, 2021, **60**, 10910–10918.
- J. Fu, Y. Yang and J.-S. Hu, *ACS Mater. Lett.*, 2021, **3**, 1468–1476.
- Y. Tanabe and Y. Nishibayashi, *Chem. Soc. Rev.*, 2021, **50**, 5201–5242.
- M. J. Chalkley, M. W. Drover and J. C. Peters, *Chem. Rev.*, 2020, **120**, 5582–5636.
- D. V. Yandulov and R. R. Schrock, *Science*, 2003, **301**, 76–78.

- 15 K. Arashiba, Y. Miyake and Y. Nishibayashi, *Nat. Chem.*, 2011, **3**, 120–125.
- 16 J. S. Anderson, J. Rittle and J. C. Peters, *Nature*, 2013, **501**, 84–87.
- 17 S. Kuriyama, K. Arashiba, K. Nakajima, Y. Matsuo, H. Tanaka, K. Ishii, K. Yoshizawa and Y. Nishibayashi, *Nat. Commun.*, 2016, **7**, 12181.
- 18 S. Kuriyama, K. Arashiba, H. Tanaka, Y. Matsuo, K. Nakajima, K. Yoshizawa and Y. Nishibayashi, *Angew. Chem. Int. Ed.*, 2016, **55**, 14291–14295.
- 19 J. Fajardo and J. C. Peters, *J. Am. Chem. Soc.*, 2017, **139**, 16105–16108.
- 20 L. R. Doyle, A. J. Wooles, L. C. Jenkins, F. Tuna, E. J. L. McInnes and S. T. Liddle, *Angew. Chem. Int. Ed.*, 2018, **57**, 6314–6318.
- 21 Y. Sekiguchi, K. Arashiba, H. Tanaka, A. Eizawa, K. Nakajima, K. Yoshizawa and Y. Nishibayashi, *Angew. Chem. Int. Ed.*, 2018, **57**, 9064–9068.
- 22 M. J. Dorantes, J. T. Moore, E. Bill, B. Mienert and C. C. Lu, *Chem. Commun.*, 2020, **56**, 11030–11033.
- 23 F. Meng, S. Kuriyama, H. Tanaka, A. Egi, K. Yoshizawa and Y. Nishibayashi, *Angew. Chem. Int. Ed.*, 2021, **60**, 13906–13912.
- 24 K. Arashiba, A. Eizawa, H. Tanaka, K. Nakajima, K. Yoshizawa and Y. Nishibayashi, *Bull. Chem. Soc. Jpn.*, 2017, **90**, 1111–1118.
- 25 K. Arashiba, H. Tanaka, K. Yoshizawa and Y. Nishibayashi, *Chem. – Eur. J.*, 2020, **26**, 13383–13389.
- 26 Y. Ashida, K. Arashiba, K. Nakajima and Y. Nishibayashi, *Nature*, 2019, **568**, 536–540.
- 27 C. E. Laplaza and C. C. Cummins, *Science*, 1995, **268**, 861–863.
- 28 C. E. Laplaza, M. J. A. Johnson, J. C. Peters, A. L. Odom, E. Kim, C. C. Cummins, G. N. George and I. J. Pickering, *J. Am. Chem. Soc.*, 1996, **118**, 8623–8638.
- 29 S. J. K. Forrest, B. Schluschaß, E. Y. Yuzik-Klimova and S. Schneider, *Chem. Rev.*, 2021, **121**, 6522–6587.
- 30 Q. J. Bruch, G. P. Connor, N. D. McMillion, A. S. Goldman, F. Hasanayn, P. L. Holland and A. J. M. Miller, *ACS Catal.*, 2020, 10826–10846.
- 31 T. J. Hebden, R. R. Schrock, M. K. Takase and P. Müller, *Chem. Commun.*, 2012, **48**, 1851.
- 32 I. Klopsch, M. Finger, C. Würtele, B. Milde, D. B. Werz and S. Schneider, *J. Am. Chem. Soc.*, 2014, **136**, 6881–6883.
- 33 T. Miyazaki, H. Tanaka, Y. Tanabe, M. Yuki, K. Nakajima, K. Yoshizawa and Y. Nishibayashi, *Angew. Chem. Int. Ed.*, 2014, **53**, 11488–11492.
- 34 Q. Liao, A. Cavallé, N. Saffon-Merceron and N. Mézailles, *Angew. Chem. Int. Ed.*, 2016, **55**, 11212–11216.
- 35 G. A. Silantyev, M. Förster, B. Schluschaß, J. Abbenseth, C. Würtele, C. Volkmann, M. C. Holthausen and S. Schneider, *Angew. Chem. Int. Ed.*, 2017, **56**, 5872–5876.
- 36 M. Pucino, F. Allouche, C. P. Gordon, M. Wörle, V. Mougél and C. Copéret, *Chem. Sci.*, 2019, **10**, 6362–6367.
- 37 F. Schendzielorz, M. Finger, J. Abbenseth, C. Würtele, V. Krewald and S. Schneider, *Angew. Chem. Int. Ed.*, 2019, **58**, 830–834.
- 38 B. Schluschaß, J. Abbenseth, S. Demeshko, M. Finger, A. Franke, C. Herwig, C. Würtele, I. Ivanovic-Burmazovic, C. Limberg, J. Telsler and S. Schneider, *Chem. Sci.*, 2019, **10**, 10275–10282.
- 39 A. Katayama, T. Ohta, Y. Wasada-Tsutsui, T. Inomata, T. Ozawa, T. Ogura and H. Masuda, *Angew. Chem. Int. Ed.*, 2019, **58**, 11279–11284.
- 40 Q. J. Bruch, G. P. Connor, C.-H. Chen, P. L. Holland, J. M. Mayer, F. Hasanayn and A. J. M. Miller, *J. Am. Chem. Soc.*, 2019, **141**, 20198–20208.
- 41 R. S. van Alten, F. Wätjen, S. Demeshko, A. J. M. Miller, C. Würtele, I. Siewert and S. Schneider, *Eur. J. Inorg. Chem.*, 2020, **2020**, 1402–1410.
- 42 B. Schluschaß, J.-H. Bortler, S. Rupp, S. Demeshko, C. Herwig, C. Limberg, N. A. Maciulis, J. Schneider, C. Würtele, V. Krewald, D. Schwarzer and S. Schneider, *JACS Au*, 2021, **1**, 879–894.
- 43 C. R. Clough, J. B. Greco, J. S. Figueroa, P. L. Diaconescu, W. M. Davis and C. C. Cummins, *J. Am. Chem. Soc.*, 2004, **126**, 7742–7743.
- 44 J. S. Figueroa, N. A. Piro, C. R. Clough and C. C. Cummins, *J. Am. Chem. Soc.*, 2006, **128**, 940–950.
- 45 J. J. Curley, E. L. Seats and C. C. Cummins, *J. Am. Chem. Soc.*, 2006, **128**, 14036–14037.
- 46 I. Klopsch, M. Kinauer, M. Finger, C. Würtele and S. Schneider, *Angew. Chem. Int. Ed.*, 2016, **55**, 4786–4789.
- 47 M. M. Guru, T. Shima and Z. Hou, *Angew. Chem. Int. Ed.*, 2016, **55**, 12316–12320.
- 48 I. Klopsch, F. Schendzielorz, C. Volkmann, C. Würtele and S. Schneider, *Z. Für Anorg. Allg. Chem.*, 2018, **644**, 916–919.
- 49 R. A. Eikey and M. M. Abu-Omar, *Coord. Chem. Rev.*, 2003, **243**, 83–124.
- 50 W. A. Nugent and B. L. Haymore, *Coord. Chem. Rev.*, 1980, **31**, 123–175.
- 51 C. Khosla, A. B. Jackson, P. S. White and J. L. Templeton, *Inorganica Chim. Acta*, 2011, **369**, 19–31.
- 52 D. Watanabe, S. Gondo, H. Seino and Y. Mizobe, *Organometallics*, 2007, **26**, 4909–4920.
- 53 A. W. Addison, T. N. Rao, J. Reedijk, J. van Rijn and G. C. Verschoor, *J. Chem. Soc., Dalton Trans.*, 1984, 1349–1356.
- 54 L. Manojlović-Muir and K. W. Muir, *J. Chem. Soc. Dalton Trans.*, 1972, 686–690.
- 55 J. Song, Q. Liao, X. Hong, L. Jin and N. Mézailles, *Angew. Chem. Int. Ed.*, 2021, **60**, 12242–12247.
- 56 A. J. Martínez-Martínez and A. S. Weller, *Dalton Trans.*, 2019, **48**, 3551–3554.
- 57 D. V. Yandulov and R. R. Schrock, *Can. J. Chem.*, 2005, **83**, 341–357.
- 58 CrysAlisPro: Data Collection and Processing Software, Rigaku Corp., Tokyo, Japan, 2015.
- 59 CrystalStructure 4.3: Crystal Structure Analysis Package, Rigaku Corp., Tokyo, Japan, 2000–2019.
- 60 G. M. Sheldrick, *Acta Crystallogr., Sect. A: Found. Adv.*, 2008, **64**, 112–122.
- 61 G. M. Sheldrick, *Acta Crystallogr., Sect. A: Found. Adv.*, 2015, **71**, 3–8.
- 62 G. M. Sheldrick, *Acta Crystallogr., Sect. C: Struct. Chem.*, 2015, **71**, 3–8.